

# Realization of deterministic 3-qubit quantum Toffoli gate with a single photon

Feiran Wang,<sup>1</sup> Shihao Ru,<sup>2</sup> Yunlong Wang,<sup>2,\*</sup> Min An,<sup>2</sup> Pei Zhang,<sup>2</sup> and Fuli Li<sup>2</sup>

<sup>1</sup>*School of Science of Xi'an Polytechnic University, Xi'an 710048, China*

<sup>2</sup>*Shaanxi Key Laboratory of Quantum Information and Quantum Optoelectronic Devices, School of Physics of Xi'an Jiaotong University, Xi'an 710049, China*

Optimizing the physical realization of quantum gates is important to build a quantum computer. Fredkin gate, also named controlled-swap gate, can be widely applicable in various quantum information processing schemes. In the present research, we propose and experimentally implement quantum Fredkin gate in a single-photon hybrid-degrees-of-freedom system. Polarization is used as the control qubit, and SWAP operation is achieved in a four-dimensional Hilbert space spanned by photonic orbital angular momentum. The effective conversion rate  $\mathcal{P}$  of the quantum Fredkin gate in our experiment is  $(95.4 \pm 2.6)\%$ . Besides, we find that a kind of Greenberger-Horne-Zeilinger states can also be prepared by using our quantum Fredkin gate, and the Mermin inequality test shows its quantum contextual characteristic. Our experimental design paves the way for quantum computing and quantum fundamental study in high-dimensional and hybrid coding quantum systems.

## I. INTRODUCTION

Universal quantum computing can be realized with a series of basic quantum gates, including phase shift gate and Hadamard gate of single qubits and controlled NOT gate of two qubits [1–5]. The multi-qubit gates, such as Fredkin (controlled SWAP) gate and Toffoli gate, can be decomposed by a set of single-qubit and two-qubit gates [6, 7]. However, the inefficient synthesis of such multi-qubit gates increases the length and time scales of quantum system, and makes the gates further susceptible to their environment. In other words, although basic quantum gates have been realized in many physical platforms and salient features of a quantum computer have been exhibited in proof-of-principle experiments [8–10], difficulties of complex operations will emerge for scaling quantum systems. The Fredkin gate is one of the typical examples. Although there exist various theoretical proposals and experimental realizations of Fredkin gate in linear optics [11], those need post-selection strategies or are probabilistic. The corresponding quantum implementation is not simple enough.

Therefore, achieving multi-qubit gates with less decoherence and less error rate by utilizing quantum resources as less as possible is key to quantum information processing. There are mainly two tactics to solve it. One is to exploit a system with accessible high dimensional states (qudits) in quantum information processing [12–14]. A qudit can be seen as a quantum particle which is not limited to two levels but in principle can have any number of discrete levels. Additionally, Using a high-dimensional system to encode qubits or realize quantum logic gates, the interaction and decoherence between multi qubits would be more less. Meanwhile qudits exhibit many merits such as enhancing channel capacities, the fault tolerance and noise resistant [15–17]. Another one is to encode qubits in multiple degrees of freedom (DoF) of a quantum

system. Even if extra DoFs, mostly, are used as auxiliary qubits, but can be directly used as computational qubits in some quantum information processing.

Furthermore, the orbital angular momentum (OAM), due to its high-dimensional quantum properties, various effective control and identification technologies, has attracted widespread attention [18]. From the perspective of quantum mechanics, the OAM occurs in discrete steps of  $\ell\hbar$ , where  $\ell$  is an unbounded integer in principle. The basic characteristic of photons carrying OAM is the existence of the spiral phase factor  $\exp(i\ell\phi)$ , where  $\phi$  is the azimuthal coordinate in the plane transverse to the propagation direction.

In this letter, we focus on the experimental realization of deterministic quantum Fredkin gate with hybrid DoFs of a single photon. Polarization and OAM DoFs are used to span the Hilbert space  $\mathcal{H}_8 = \mathcal{H}_2^P \otimes \mathcal{H}_4^O$ , where the subscripts represent the corresponding spatial dimension. A series of quantum states are inputted to illustrate the performance of the Fredkin gate. Not only are the conversion rate used, but also do we have quantum state tomography (QST) in Hilbert space  $\mathcal{H}_4^O$  while the polarization of a given quantum state is horizontal, vertical or diagonal. All conversion rates measured are greater than 93%. In addition, a kind of Greenberger-Horne-Zeilinger (GHZ) states can be generated by our quantum Fredkin gate, and we perform a Mermin inequality test to discuss its quantum contextuality. Our research paves the way for quantum computing and quantum fundamental study by using hybrid-DoF or high-dimension coding methods.

## II. EXPERIMENTAL SETUP

The Fredkin gate has been experimentally implemented with linear optics on multi-photon single-DoF system [11]. But something more meaningfully, coding in a single photon with hybrid DoFs to realize Fredkin gate is much more economical than a multi-photon single-DoF coding method. As will be described below, our experimental proposal is deterministic and there is no photon

\* [yunlong.wang@mail.xjtu.edu.cn](mailto:yunlong.wang@mail.xjtu.edu.cn)

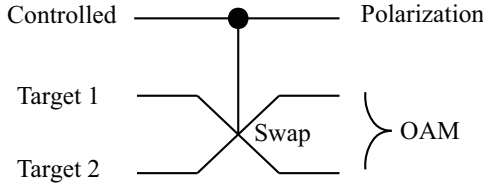


FIG. 1. The quantum Fredkin gate circuit. The control qubit is encoded by polarization DoF ( $|V\rangle \rightarrow |0\rangle$  and  $|H\rangle \rightarrow |1\rangle$ ), and the two target qubits are encoded in a four-dimensional Hilbert space spanned by OAM states from  $|\ell = -2\rangle$  to  $|\ell = +1\rangle$ , of which specific coding methods are  $|\ell = -1\rangle \rightarrow |00\rangle$ ,  $|\ell = -2\rangle \rightarrow |01\rangle$ ,  $|\ell = 0\rangle \rightarrow |10\rangle$  and  $|\ell = +1\rangle \rightarrow |11\rangle$ .

loss in theory. The Fredkin gate can be written as

$$U_{\text{Fred}} = |0\rangle\langle 0| \otimes I_4 + |1\rangle\langle 1| \otimes U_{\text{SWAP}}.$$

As shown in Fig. 1, it is a three-qubit controlled-swap gate, that is, conditioned on the state of the control qubit, the states of the two target qubits are swapped.

Figure 2 illustrates our linear optical scheme for the quantum Fredkin gate. The OAM space is from  $|\ell = -2\rangle$  to  $|\ell = +1\rangle$  here, and any arbitrary superposition OAM states can be generated by spatial light modulator (SLM). The half wave plate (HWP) and quarter wave plate (QWP) positioned behind SLM1 also module an arbitrary polarization quantum state of the control qubit. The core component of our experimental scheme is an altered Mach-Zehnder interferometer composed of parts (a)-(c), time delay, and two PBSs before and after them in Fig. 2. Polarized beamer splitters 1 and 2 (PBS) are used as controlled operation for polarization DoF. The computational state  $|1\rangle$  of the control qubit corresponds to the horizontal polarization photon propagating in the upper interferometer arm, while the state  $|0\rangle$  is represented by vertical polarization photon propagating in the lower arm of the polarization Mach-Zehnder interferometer. The time-delay part in the lower arm is used to balance the path difference between two arms.

Notice that the part (a) and part (c) are identity in the experimental settings. All the angles of HWPs are at  $\pi/8$  and  $3\pi/8$ , sequentially, and the angles of Dove primes are at  $\pi/4$ . In general, if the Dove Prism is rotated by an angle of  $\alpha$ , the OAM mode can be operated in the following manner,

$$|l\rangle \xrightarrow{\text{Dove}} i \exp(i2\ell\alpha) | -l \rangle.$$

While the forward propagating photon in an OAM state  $|l\rangle$  would be added a phase of  $\exp(i2\ell\alpha)$ , the backward propagating photon carrying the same OAM mode would be added an opposite phase of  $\exp(-i2\ell\alpha)$ . The embedded Sagnac interferometers (scilicet the part(a) and (c)) label as parity sorters, are designed to distinguish photons based on the parity of its OAM quantum numbers. Strictly speaking, this kind of parity sorter can be used to constitute quantum non-demolition measurement in hyperentangled Bell states measurement.

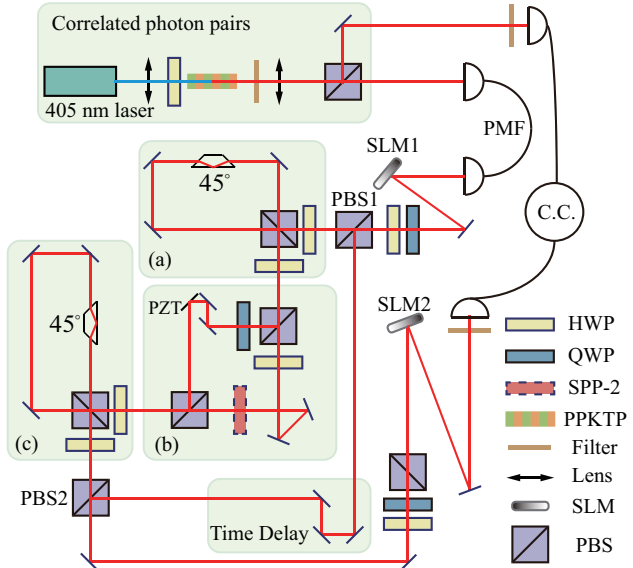


FIG. 2. Quantum Fredkin gate for three qubits encoded into SAM and OAM DoFs of a single photon. A continuous wave laser with average power of 12 mW at 405 nm pumps a nonlinear crystal of PPKTP cut for degenerate type II non-collinear phase matching which emits correlated photon pairs at 810 nm. Photons from the source are spatially filtered to the fundamental Gaussian mode using a PMF. The vertical photon from correlated photon source is directly coupled into PMF and detected by SPAD as a trigger signal. SLM1, a reflector and a set of plates are used to separately modulate traverse and polarization modes of another photon. Part (a)-(c) and the two PBSs before and after them is to achieve the quantum Fredkin gate here. The combination of QWP, HWP and PBS is to modulate the polarization modes of photons to the horizontal polarization, which is responded by SLM2, and the tomography of OAM Hilbert space  $\mathcal{H}_4$  is performed with SLM2. The phase of this photon is flattened, coupled into PMF and detected by another SPAD. PPKTP: periodically poled potassium titanyl phosphate; HWP: half wave plate; QWP: quarter wave plate; PBS: polarizing beam splitter; SLM: spatial light modulator; SPP: spiral phase plate; PZT: piezoelectric transducer; PMF: polarization maintaining single mode fiber; SPAD: single-photon avalanche detector.

The part (b), also a Mach-Zehnder interferometer in which odd spatial mode photons propagate in upper arm and even spatial mode propagate in lower arm, is to swap the even modes  $|\ell = 0\rangle$  and  $|\ell = -2\rangle$  themselves by using a spiral phase plate (SPP). Meanwhile, we add a QWP at  $0^\circ$  and a HWP at  $\pi/2$  in part (b) to compensate the phase induced by the overall reflection number on the relative phase between odd and even modes. A PZT in the upper arm combined with a motorized translation stage is to ensure the optical path of two arm same. That is, no additional phase is introduced. Based on the above modules, we can experimentally implement the Fredkin gate with hybrid DoFs.

In order to explain more clearly, assume that the OAM

initial state is generated by SLM1 as follows,

$$|\psi_1\rangle = |H\rangle \otimes (C_{-2}| - 2\rangle + C_{-1}| - 1\rangle + C_0|0\rangle + C_{+1}| + 1\rangle),$$

where  $\sum_{i=-2}^1 |C_i|^2 = 1$ . After a reflector, a QWP and a HWP, it becomes

$$|\psi_2\rangle = i(\cos \alpha |H\rangle + e^{i\beta} \sin \alpha |V\rangle) \otimes (C_{-2}| + 2\rangle + C_{-1}| + 1\rangle + C_0|0\rangle + C_{+1}| - 1\rangle).$$

Here we consider the situation of the upper and the lower arms, respectively. Only some mirrors are included in the lower arm for a time delay. Therefore, the quantum state of photon propagating through the lower arm can be written as

$$|\psi_d\rangle = -e^{i\beta} \sin \alpha |V\rangle \otimes (C_{-2}| - 2\rangle + C_{-1}| - 1\rangle + C_0|0\rangle + C_{+1}| + 1\rangle) \quad (1)$$

after PBS2. For the upper arm, we consider that the four different OAM spatial modes transform through part (a), (b), and (c). As mentioned above, the quantum state is transferred into

$$|\psi_u\rangle = -\cos \alpha |H\rangle \otimes (C_{-2}|0\rangle + C_{-1}| - 1\rangle + C_0| - 2\rangle + C_{+1}| + 1\rangle). \quad (2)$$

Comparing Eq. (1) with Eq. (2), one can see that no extra relative phase of quantum states is added between the two arms and the global phase can be ignored. Besides, recall that our coding methods of four-dimensional OAM Hilbert space are  $|l = -1\rangle \rightarrow |00\rangle$ ,  $|l = -2\rangle \rightarrow |01\rangle$ ,  $|l = 0\rangle \rightarrow |10\rangle$  and  $|l = +1\rangle \rightarrow |11\rangle$ , that is, two qubits can be encoded with a four-dimensional OAM qudit,  $\mathcal{H}_4^o = \mathcal{H}_2 \otimes \mathcal{H}_2$ . Therefore, using Eq. (1) and Eq. (2), the final quantum state becomes

$$\begin{aligned} |\psi_f\rangle &= |\psi_u\rangle + |\psi_d\rangle \\ &= (|0\rangle\langle 0| \otimes I_4 + |1\rangle\langle 1| \otimes U_{\text{SWAP}}) |\psi_2\rangle \\ &= U_{\text{Fred}} |\psi_2\rangle. \end{aligned}$$

That is to satisfy the quantum Fredkin gate.  $\blacksquare$

### III. RESULT AND ANALYSIS

For measurements, we adopt the crosstalk measurements between the input and output states in the computational basis and perform the QST for the output states in the OAM Hilbert space. The computational basis includes the eight eigenstates (from  $|000\rangle$  to  $|111\rangle$ ) of  $\sigma_z$ . Experimentally, a set of wave plates and a SLM can achieve computational basis measurements in polarization and OAM hybrid DoFs, and this setup can also be used for QST.

To exhibit the quality of the Fredkin gate, we define the effective conversion rate  $\mathcal{P}$  for the transformation,

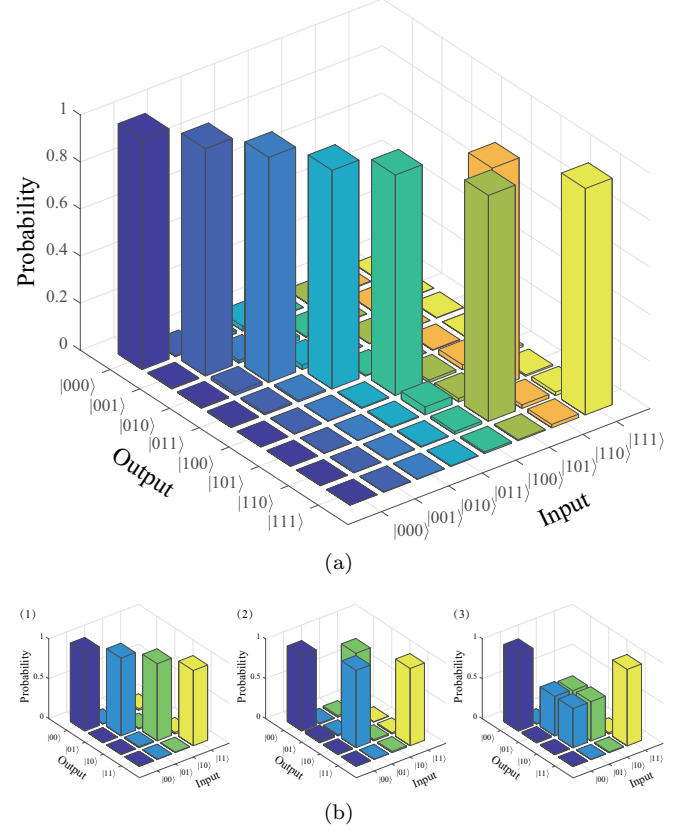


FIG. 3. Truth tables of the Fredkin gate. (a) After preparing three qubits in one of the eight basis input states from  $|000\rangle$  to  $|111\rangle$ , the probabilities of all basis output states are measured 1 minute. (b) For supplementary explanation, the subgraphs are the truth tables corresponding to the target qubits while the state of control qubit is  $|0\rangle$ ,  $|1\rangle$  and  $(|0\rangle+|1\rangle)/\sqrt{2}$ , respectively.

according to  $\mathcal{P}(i, j) = N_{ij} / \sum_{mn} N_{mn}$ , where  $N_{ij}$  corresponds to the coincidence count entries in the diagonal crosstalk matrix. It is obtained from the crosstalk measurements between the input and output modes.

The truth table depicted in Fig. 3(a) shows the probabilities of all computational basis states after applying the Fredkin gate to each of the computational basis states. The effective conversion rate of the truth table is  $\mathcal{P} = (95.4 \pm 2.6)\%$ . For more detailed classification, we measured the outputs of the gate for each of the four possible computational basis input states ( $|00\rangle$ ,  $|01\rangle$ ,  $|10\rangle$  and  $|11\rangle$ ) while control qubit 1 is being in the different states. If the state of control qubit is  $|0\rangle$ , Fig. 3(b)-(1) shows that the states of target qubits 2 and 3 indeed invariant, satisfying the theoretical prediction. Figure 3(b)-(2) shows that the unitary transformation of qubits 2 and 3 actually is a SWAP gate if control qubit is in the state  $|1\rangle$ . The effective conversion rate of this SWAP gate is  $\mathcal{P}_{\text{SWAP}} = 95.9\%$ . These reveal the characteristic properties of the Fredkin gate, named that a SWAP operation is applied on the two target qubits if the control qubit is in the state  $|1\rangle$ . In addition, in order to manifest well coher-

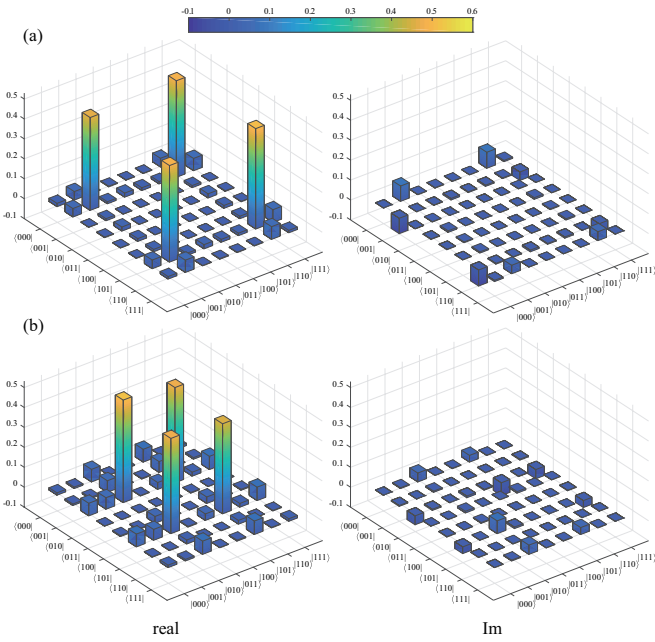


FIG. 4. The reconstructed density matrices for two GHZ states. The control and two target qubits are measured in the  $D/A$  basis ( $\sigma_x$ ); in the  $R/L$  basis ( $\sigma_y$ ); and in the  $H/V$  basis ( $\sigma_z$ ). Part (a) is  $|\text{GHZ}_1\rangle$  and part (b) is  $|\text{GHZ}_2\rangle$ .

ence of our experimental setup, we consider the situation where the control qubit is in the state  $(|0\rangle + |1\rangle)/\sqrt{2}$  and the gate is in a superposition of the SWAP and identity operations. The results are shown in Fig. 3(b)-(3).

Furthermore, using our Fredkin gate, one can produce maximally entangled three-qubit states, GHZ states  $|\psi_{\mu\lambda\omega}\rangle = \sum_{j=0,1} (-1)^{\mu j} |j, j \oplus \lambda, j \oplus \omega\rangle/\sqrt{2}$ , in which  $\mu, \lambda, \omega, j$  vary 0 or 1. Two states  $|\text{GHZ}_1\rangle$  ( $|\psi_{001}\rangle$ ) and  $|\text{GHZ}_2\rangle$  ( $|\psi_{010}\rangle$ ) are illustrated in Fig. 4, namely,

$$(|0\rangle + |1\rangle)|01\rangle/\sqrt{2} \xrightarrow{\text{Fredkin}} |\text{GHZ}_1\rangle : (|001\rangle + |110\rangle)/\sqrt{2},$$

$$(|0\rangle + |1\rangle)|10\rangle/\sqrt{2} \xrightarrow{\text{Fredkin}} |\text{GHZ}_2\rangle : (|010\rangle + |101\rangle)/\sqrt{2}.$$

A full state reconstruction can be carried out by a set of 27 measurements setting  $(\sigma_x\sigma_x\sigma_x, \sigma_x\sigma_x\sigma_y, \dots, \sigma_z\sigma_z\sigma_z)$ , effectively resulting in an overcomplete set of 216 projective measurements. Figure 4 shows the real and imagine parts of the reconstructed density matrices of the two GHZ states, which we used a maximum-likelihood algorithm to get. We measure the fidelity between the output state  $\varrho_o$  and the desired state  $\varrho_e$  as  $F(\varrho_o, \varrho_e) = (\text{Tr} \sqrt{\sqrt{\varrho_o}\varrho_e\sqrt{\varrho_o}})^2$ , and obtain  $F = (96.8 \pm 2.3)\%$  for  $|\text{GHZ}_1\rangle$  and  $F = (96.0 \pm 1.7)\%$  for  $|\text{GHZ}_2\rangle$ . The errors

TABLE I. The correlation functions values of  $|\text{GHZ}_1\rangle$ .

$\langle \sigma_x\sigma_x \cdot \sigma_x \rangle$	$\langle \sigma_x\sigma_y \cdot \sigma_y \rangle$	$\langle \sigma_y\sigma_x \cdot \sigma_y \rangle$	$\langle \sigma_y\sigma_y \cdot \sigma_x \rangle$
$0.970 \pm 0.014$	$0.942 \pm 0.010$	$0.944 \pm 0.016$	$-0.962 \pm 0.011$

are calculated using Monte Carlo simulations from our measurement sampling.

For quantum fundamental research, we can perform further measurements to characterize the quantum contextuality of the state  $|\text{GHZ}_1\rangle$  [19]. GHZ states can be used to show a strong contradiction between the hidden variable theories and quantum mechanics. In experiment, we use a kind of Bell-like inequalities to study this contradictory phenomenon. This Bell-like inequality or named Mermin inequality can be written as

$$S_M = \left| \langle \sigma_x\sigma_x \cdot \sigma_x \rangle + \langle \sigma_x\sigma_y \cdot \sigma_y \rangle \right. \\ \left. + \langle \sigma_y\sigma_x \cdot \sigma_y \rangle - \langle \sigma_y\sigma_y \cdot \sigma_x \rangle \right| \leq 2,$$

which holds for any hidden variable theories since each of the six variables are assigned to predefined values  $+1$  or  $-1$ . However, quantum mechanics predicts the maximal value of the computation to be 4 (with ideal equipments). We calculate it from the QST results of  $|\text{GHZ}_1\rangle$ , and the corresponding correlation functions are listed in TABLE I. The expectation value of  $S_M$  in our experiment can be obtained as  $3.818 \pm 0.016$ . This value is greater than the maximum predicted under the hidden variable theories background. Therefore, it actually discards that hidden variable theories are extensions of quantum mechanics.

#### IV. CONCLUSION

In summary, an efficient method to construct quantum Fredkin gate with hybrid DoFs of a single photon is presented in this scheme. Using the polarization DoFs and the four-dimensional OAM space to encode the control bit and the two target bits respectively, we implemented a deterministic optical Fredkin gate without photon loss. This coding method can also be extended to  $n$ -bit Fredkin gate, and can be used to implement CNOT gate and Toffoli gate. Additionally, we prepared a single-photon multi-DoF GHZ state through the Fredkin gate and tested its violation of Mermin's inequality, which can rule out the predictions of noncontextual hidden variable theory.

#### ACKNOWLEDGMENTS

This work is supposed by the the National Natural Science Foundation of China (Grant Nos. 11534008, 11804271 and 91736104), Ministry of Science and Technology of China (2016YFA0301404) and China Postdoctoral Science Foundation via Project No. 2020M673366.

---

[1] Adriano Barenco, Charles H. Bennett, Richard Cleve, David P. DiVincenzo, Norman Margolus, Peter Shor, Tycho Sleator, John A. Smolin, and Harald Weinfurter, “Elementary gates for quantum computation,” *Phys. Rev. A* **52**, 3457–3467 (1995).

[2] Sergey Bravyi and Alexei Kitaev, “Universal quantum computation with ideal clifford gates and noisy ancillas,” *Phys. Rev. A* **71**, 022316 (2005).

[3] Philip Walther, Kevin J Resch, Terry Rudolph, Emmanuel Schenck, Harald Weinfurter, Vlatko Vedral, Markus Aspelmeyer, and Anton Zeilinger, “Experimental one-way quantum computing,” *Nature* **434**, 169–176 (2005).

[4] Jeremy L O’brien, “Optical quantum computing,” *Science* **318**, 1567–1570 (2007).

[5] S Takeda and A Furusawa, “Toward large-scale fault-tolerant universal photonic quantum computing,” *APL Photonics* **4**, 060902 (2019).

[6] John A. Smolin and David P. DiVincenzo, “Five two-bit quantum gates are sufficient to implement the quantum fredkin gate,” *Phys. Rev. A* **53**, 2855–2856 (1996).

[7] Nengkun Yu, Runyao Duan, and Mingsheng Ying, “Five two-qubit gates are necessary for implementing the toffoli gate,” *Phys. Rev. A* **88**, 010304 (2013).

[8] Pieter Kok, William J Munro, Kae Nemoto, Timothy C Ralph, Jonathan P Dowling, and Gerard J Milburn, “Linear optical quantum computing with photonic qubits,” *Reviews of Modern Physics* **79**, 135 (2007).

[9] Jeremy L O’brien, Akira Furusawa, and Jelena Vučković, “Photonic quantum technologies,” *Nature Photonics* **3**, 687–695 (2009).

[10] Thaddeus D Ladd, Fedor Jelezko, Raymond Laflamme, Yasunobu Nakamura, Christopher Monroe, and Jeremy Lloyd O’Brien, “Quantum computers,” *Nature* **464**, 45–53 (2010).

[11] Raj B Patel, Joseph Ho, Franck Ferreyrol, Timothy C Ralph, and Geoff J Pryde, “A quantum fredkin gate,” *Science advances* **2**, e1501531 (2016).

[12] Manuel Erhard, Robert Fickler, Mario Krenn, and Anton Zeilinger, “Twisted photons: new quantum perspectives in high dimensions,” *Light: Science & Applications* **7**, 17146–17146 (2018).

[13] Andrew Forbes and Isaac Nape, “Quantum mechanics with patterns of light: Progress in high dimensional and multidimensional entanglement with structured light,” *AVS Quantum Science* **1**, 011701 (2019).

[14] Manuel Erhard, Mario Krenn, and Anton Zeilinger, “Advances in high-dimensional quantum entanglement,” *Nature Reviews Physics* , 1–17 (2020).

[15] Nicolas J. Cerf, Mohamed Bourennane, Anders Karlsson, and Nicolas Gisin, “Security of quantum key distribution using  $d$ -level systems,” *Phys. Rev. Lett.* **88**, 127902 (2002).

[16] Hoi-Kwong Lo, Marcos Curty, and Kiyoshi Tamaki, “Secure quantum key distribution,” *Nature Photonics* **8**, 595–604 (2014).

[17] Sebastian Ecker, Frédéric Bouchard, Lukas Bulla, Florian Brandt, Oskar Kohout, Fabian Steinlechner, Robert Fickler, Mehul Malik, Yelena Guryanova, Rupert Ursin, and Marcus Huber, “Overcoming noise in entanglement distribution,” *Phys. Rev. X* **9**, 041042 (2019).

[18] Yijie Shen, Xuejiao Wang, Zhenwei Xie, Changjun Min, Xing Fu, Qiang Liu, Mali Gong, and Xiaocong Yuan, “Optical vortices 30 years on: Oam manipulation from topological charge to multiple singularities,” *Light: Science & Applications* **8**, 1–29 (2019).

[19] Shihao Ru, Weidong Tang, Yunlong Wang, Feiran Wang, Pei Zhang, and Fuli Li, “Theoretical and experimental investigation of gauge-like equivalent quantum noncontextual inequalities,” *arXiv preprint arXiv:2010.05266* (2020), <https://arxiv.org/abs/2010.05266>.